

# Cd hyperfine fields at the bcc Fe/Co interface

V. Bellini, R. Zeller, and P. H. Dederichs

*Institut für Festkörperforschung, Forschungszentrum Jülich, D-52425 Jülich, Germany*

(Received 23 January 2001; published 24 September 2001)

We present *ab initio* calculations for the magnetic properties of the (001) and (110) bcc Fe/Co interfaces. The calculations are performed by the Korringa-Kohn-Rostoker Green's-function method using the local-density approximation of density-functional theory. Of central interest is the relation between the hyperfine fields induced on substitutional Cd probe atoms and the magnetization profile at the interface. We compare the calculated Cd hyperfine fields with the ones measured by a time-differential perturbed angular correlation spectroscopic experiment [B. Swinnen, J. Meersschaet, J. Dekoster, G. Langouche, S. Cottenier, S. Demuyne, and M. Rots, *Phys. Rev. Lett.* **78**, 362 (1997)]. The comparison suggests that the considered interfaces between Fe and Co are strongly interdiffused, so that no "simplified" relation exists between the measured hyperfine fields and the magnetic moments at the interface.

DOI: 10.1103/PhysRevB.64.144427

PACS number(s): 75.70.Cn, 75.50.Bb

## I. INTRODUCTION

The study of the hyperfine interactions in solids received considerable attention in the last decades both from the experimental and theoretical side because they provide unique microscopic information about the structural as well as magnetic properties of low-dimensional magnetic systems such as surfaces, interfaces, and dilute alloys.<sup>1–5</sup> The hyperfine properties arise from the magnetic dipole or electric quadrupole interaction between the nuclear moment and the external electromagnetic field due to the electrons, and result in an energy splitting of the nuclear levels. Experimental techniques differ depending whether they make use of resonance effects working in the "energy domain" measuring directly the energy splittings, e.g., Mössbauer effect or nuclear magnetic resonance (NMR) experiments, or whether they work in the "time domain" measuring the precession frequency of the nuclear spins by means of the  $\gamma$  radiation emitted by radioactive nuclei, as it is the case in the perturbed-angular-correlation (PAC) spectroscopy.

Since the information that is supplied by these type of experiments is often very difficult to interpret and far from transparent, reliable theoretical calculations are very much needed in order to provide a theoretical basis for the understanding of the experimental quantities. *Ab initio* calculations for the hyperfine interactions in solids have shown in the past to be well suited for this scope, and have succeeded to reproduce, and explain, qualitatively and often also quantitatively, experiments on, e.g., dilute ferromagnetic alloys,<sup>6–8</sup> hcp metals<sup>9</sup> and defects in semiconductors.<sup>10,11</sup>

In the same time the techniques for crystal growth are refined so much that systems like interfaces and overlayers on metals can be constructed with high accuracy, and new metastable crystallographic phases can be obtained. One interesting achievement in this respect was reported by Prinz<sup>12</sup> who succeeded to stabilize Co grown on (110) GaAs in the exotic bcc structure, while in the bulk it prefers the hcp structure (up to  $T=425$  K where it transforms into fcc). The *hyperfine fields*, arising from the interaction between the nuclear magnetic dipole of a probe atom and the surrounding magnetization, might hence be of great help to characterize

these new phases since they act as fingerprints of the crystal structure and magnetic environment in which the nucleus of the probe atom under consideration is embedded.

This work was motivated by a recent paper of Swinnen *et al.*<sup>13</sup> where the hyperfine fields of Cd impurity probe atoms implanted in (1–10) bcc Fe/Co multilayers grown by molecular beam epitaxy were measured by means of a time-differential PAC spectroscopy. Using a fitting procedure based on a model by Stearns,<sup>14</sup> the magnetic moment profile at the Fe/Co interface is deduced from the measured hyperfine field satellites and an oscillatory behavior of both the Fe and Co moments in the interface region is predicted. As was already pointed out by other authors,<sup>15,16</sup> *ab initio* calculations of the magnetic moment profile for the Fe/Co interface show instead a monotonic increase of the Fe moment towards the interface and a saturated constant value for the Co moments. This behavior is fully in line with the magnetic properties of Co impurities in bulk Fe<sup>17</sup> and with the experimental and calculated Slater-Pauling curve of disordered FeCo alloys.<sup>18</sup> A detailed discussion of the magnetic interface profiles and their relation to the corresponding disordered alloys has been recently given by Niklasson *et al.*<sup>16</sup>

In this paper we address the more challenging problem of calculating the hyperfine fields of Cd probe atoms at different sites close to the interface. Our aim is to directly compare with the Cd hyperfine fields measured by PAC experiments, in this way avoiding any unjustified assumption in the interpretation of the experimental data. This concerns, e.g., the assignment of the Cd satellites to sharp interface regions or the use of Stearns' model for the relation between the Cd hyperfine fields and the moments at the interface. The possibility of relating hyperfine fields and magnetic moments in FeCo and FeCr alloys by simple models has already been discussed by Ebert *et al.*<sup>19</sup> who came to the conclusion that such models are of limited use because the expansion coefficients change with the surroundings. The direct comparison of calculated hyperfine fields with measured fields is more fundamental and can give us a nontrivial information about the geometrical structure of the interface, whether it is sharp or weakly interdiffused, with interdiffused regions and patches of nearly sharp interfaces as it is concluded by Swinnen *et al.*,<sup>13</sup> or whether it is strongly interdiffused with no resemblance to the sharp interface, as we will conclude here.

The paper is organized as follows: In Sec. II we present details of the method used in the calculations, while in Sec. III we briefly discuss the calculated magnetization profile at the ideal Fe/Co (001) and (110) interfaces. In Sec. IV we present as our main result, the hyperfine fields of the Cd impurities at the Fe/Co (001) and (110) interfaces that are compared in Sec. V with the measured values. In Sec. VI we summarize and conclude.

## II. THE THEORY

In the present calculations we adopted the so called atomic sphere approximation for the potentials, considering them as spherical inside slightly overlapping spheres with volumes equal to the one of the Wigner-Seitz cell. Angular momenta up to  $l_{max}=3$  are considered in the expansion of the wave functions, while a multipole expansion of the charge density up to  $l=6$  is used to take the intercell contribution of the potential into account. Brillouin zones have been sampled by means of the special-point method.<sup>20,21</sup> The exchange and correlation functionals are included in the local-density approximation (LDA), with the parametrization given by Vosko, Wilk, and Nusair,<sup>22</sup> and relativistic effects are included in the scalar relativistic approximation (SRA).

### A. The screened Korringa-Kohn-Rostoker method

In order to describe the bcc Fe/Co interfaces with (001) and (110) orientations we used the screened Korringa-Kohn-Rostoker (SKKR) Green's-function method<sup>23–25</sup> for layered systems. While in the traditional KKR method the free-space Green's function is used, being long ranged and of oscillatory nature, in the screened KKR method the Green's function of a reference system is introduced, which, e.g., consists of a system of repulsive muffin-tin potentials, assumed here to have a constant height of 4 Ry. The Green's function of this repulsive system, i.e., the “screened structure constants”  $G_{LL'}^{r nn'}$ , decay exponentially in space and lead thus to a short-ranged coupling. In case of layered systems the screening property results into a  $\mathcal{N}$ -scaling effort in the solution of the Dyson equation; this is of particular importance when we have to tackle very large systems with a reasonable investment of computing time.<sup>23–25</sup>

To model the bcc Fe/Co interface we considered a slab of 5Fe/11Co/5Fe monolayers embedded between two, left and right, bcc Fe half-crystals (see Fig. (1)). We allowed the potentials of this slab to readjust self-consistently in the iterations while the Fe potentials at the two half-crystals were kept constant to their unperturbed bulk values. No lattice relaxations were included, i.e., the Fe and Co monolayers at the interface region fixed at the bulk Fe distances. This approximation, as it has been discussed by Šljivančanin and Vukajlović<sup>15</sup> influences only to a minor extent the magnetic properties at the interface, since the lattice mismatch between Fe and Co is very small; the experimental lattice constant of bcc Co observed by Prinz is 5.344 a.u. while the Fe one is 5.406 a.u. The calculation of the surface Green's functions of the two bulk Fe half-crystals is achieved by means of decimation techniques.<sup>26,27</sup>

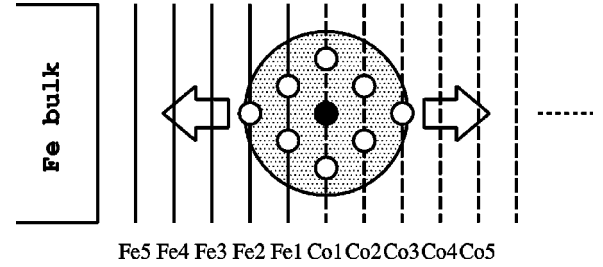


FIG. 1. An interface region composed of 5Fe/11Co/5Fe monolayers with (001) and (110) orientations is sandwiched between two bulk Fe half-crystals (in the above picture only half of the system is depicted). The arrows indicate that the Cd impurity with the cluster of perturbed neighboring potentials can be positioned in different layers at the interface.

### B. The impurity calculations

In the case of impurities calculations at the interface we use the KKR-Green's-function method for impurities.<sup>28,29</sup> In contrast to the usual calculations for impurities in the bulk, the Green's function of the ideal interface, as calculated in Sec. II A, is chosen as the reference system and only a finite number of potentials (up to the third shell sites) around the impurity are allowed to be perturbed (such a cluster is indicated by a circle in Fig. 1). The impurity is then moved across the interface region as indicated in Fig. 1 and for each position all the potentials inside the cluster are iterated until self-consistency is reached.

### C. The hyperfine fields

The correct relativistic expression for the hyperfine field has been originally derived by Breit,<sup>30</sup> and more recently rederived by Blügel *et al.*,<sup>6</sup> starting from the Dirac equation, the original expression can be uniquely split in three parts that are the relativistic generalizations of the contact, dipole, and orbital contributions to the hyperfine field. Since spin-orbit coupling is neglected in the SRA, the orbital term vanishes; moreover dipole terms are usually small. In the SRA we are thus left mainly with the contact term, or more precisely with the relativistic version of the Fermi contact term,<sup>31</sup> given by the modified Breit's formula<sup>6</sup>

$$H_{hf}^{Breit} = \frac{8\pi}{3} m_{\tau}, \quad (1)$$

where the effective magnetization density  $m_{\tau}$  near the nucleus is obtained as an average over a small region around the nucleus whose diameter is the Thomson radius  $r_T = Ze^2/mc^2$ . Since the hyperfine fields are determined by the behavior of the wave functions close to the nucleus, relativistic effects are already important for elements with relatively small nuclear charges.

There are two physically different contributions to this contact term;<sup>4,6</sup> the first one arises from the intra-atomic spin polarization of the  $s$  orbitals induced by the  $d$  orbitals at the same site, the second one from the interatomic polarization induced by the  $d$  orbitals of the neighboring atoms. The first process acts on both core and valence  $s$  orbitals, while the

second one influences only the valence  $s$  orbitals, which have sufficient spatial overlap with the neighbors. As is well known the core hyperfine field is mainly proportional to the total magnetic moment of the probe atom, while the valence hyperfine field has a more complicated behavior. Moreover, since  $sp$  impurities in ferromagnets carry only very small moments, e.g.,  $0.025\mu_B$  for a Cd impurity in Fe, the contribution to the hyperfine field from the core orbitals is small and only the valence contribution is significant, i.e., the  $sd$  interatomic polarization effect dominates; the total hyperfine field has thus mainly a “transferred” character arising from the magnetic environment in which the nonmagnetic probe atom is embedded.

The hyperfine fields (hff) induced on magnetic impurities are subjected to the well-known “core-polarization” problem<sup>6,32</sup> arising from the use of the LDA. The LDA error results in an underestimation of up to 30% in the core contribution to the hff, the valence contribution instead should not be affected by this problem. Since in this paper we deal with a nonmagnetic Cd impurity, our results are more or less free from this LDA “error.” On the other hand the hyperfine fields induced on the Cd atoms will depend on the magnitude of the magnetic moments of the neighboring Fe and Co atoms; the choice of the lattice constant may therefore, we will discuss it below, affect the results, above all because a “weak” ferromagnet like Fe is involved. In the present calculations we do not include relaxations around the Cd atoms, i.e., the Fe and Co atoms retain their ideal bcc lattice positions. For  $5sp$  impurities in Fe the relaxation of neighboring Fe atoms is expected to induce small changes for impurities at the beginning of the  $sp$  series (like Cd).<sup>7</sup>

### III. THE Fe/Co INTERFACE

For the understanding of the magnetic moment profiles at the Fe/Co interfaces it is important to recall first the behavior of bulk Co and Fe and FeCo alloys. Bulk Co is for all three phases (hcp, fcc, and bcc) a strong ferromagnet characterized by a filled majority band and a moment of about  $1.7\mu_B$ , being insensitive to structural and environmental changes. On the other hand, due to the larger extent of the wave function resulting in stronger hybridization and band broadening, bcc Fe is a weak ferromagnet with about 0.4–0.5 unoccupied  $d$  states in the majority band, leading to a strong sensitivity of the Fe moment to environmental changes. This can be clearly seen in *ab initio* calculations for disordered  $\text{Fe}_{1-x}\text{Co}_x$  alloys.<sup>18,19</sup> With increasing Co concentrations the average alloy moment increases and attains a maximum at about 25% Co, despite the fact that the Co moment, being about  $1.7\mu_B$  independently of the concentration, is much smaller than the Fe moment. Calculations for the dilute limit of a single Co impurity in Fe show, that around each Co impurity the neighboring Fe moments increase in a region of at least five Fe shells<sup>17</sup> so that for each Co atom the total alloy moment increases by about  $1\mu_B$ . All these *ab initio* calculations are in good agreement with the experimental information from magnetization measurements and neutron scattering, showing the high predictability of LDA calculations for the local moments.

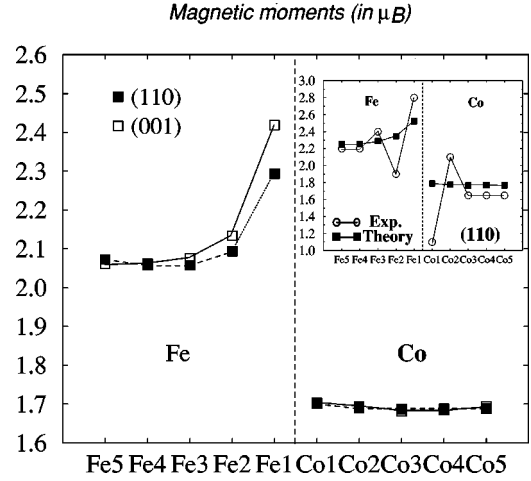


FIG. 2. Magnetic moment profiles at the (001) and (110) Fe/Co interfaces; the bcc Fe LDA lattice constant, i.e.,  $a_{\text{latt}} = 5.205$  a.u., is used. In the inset, the profile obtained using the bcc Fe experimental lattice constant, i.e.,  $a_{\text{latt}} = 5.406$  a.u., is compared with the fitted magnetic profile given by Swinnen (Ref. 13).

In analogy to the alloy, the behavior at the Fe/Co interface is characterized by the filling of the local majority  $d$  states of Fe being driven by the decrease of hybridization and the resulting band narrowing at the interface. The magnetic moment profile at the (001) and (110) Fe/Co interfaces calculated for the LDA bcc Fe lattice constant ( $a_{\text{latt}} = 5.205$  a.u.) are shown in Fig. 2, while in the inset the magnetization profile at the (110) interface obtained using the experimental Fe lattice constant ( $a_{\text{latt}} = 5.406$  a.u.) is compared with the “claimed” fitted magnetic moment profile proposed by Swinnen *et al.*<sup>13</sup> The basic feature is that no oscillatory behavior in the calculated magnetic moment profiles is found, which recalls the behavior of the single Co impurity in Fe. For both orientations the Co moment is practically constant up to the interface, while the Fe moment monotonically increases to an enhanced value at the interface, which is for (001) considerably larger than the value at the (110) interface. The differences between the (001) and (110) interface can be understood from the different coordination numbers of a Fe atom in the first Fe layer (Fe1) at the interface, having four nearest-neighbor (nn) and one next-nearest neighbor (nnn) Co atoms at the (001) interface, but only two nn and two nnn Co atoms in the (110) case. Our results are in good agreement with earlier calculations<sup>15,16</sup> obtained by different *first-principles* approaches.

From the above discussion it is clear that the conclusions of Swinnen *et al.* are obviously wrong. We will postpone the reason for this to Sec. V. Here we will proceed to directly calculate the hyperfine fields of Co probe atoms at the Fe/Co interfaces. The aim is to compare with the experimental “raw” data of Swinnen *et al.* and from this to obtain information about the real interface structure.

### IV. Cd HYPERFINE FIELDS AT THE Fe/Co INTERFACE

In Fig. 3 we show the results for the hff of a Cd probe atom placed in different layers at the Fe/Co interface for both



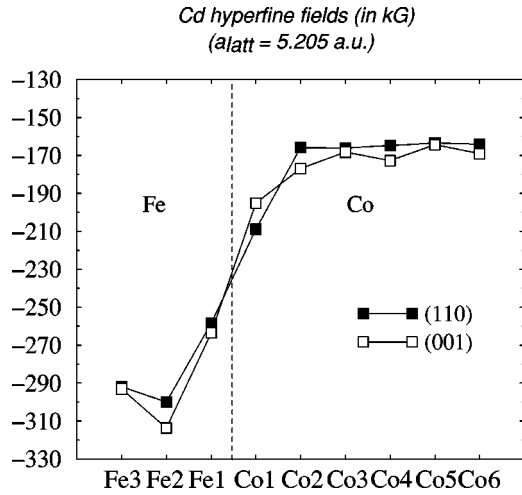


FIG. 3. Cd hff profile at the (001) (open squares) and (110) (filled squares) Fe/Co interfaces.

the (001) and (110) orientations. Here the LDA lattice constant of Fe is used and the Co layers are not relaxed. As discussed in Sec. II C, the hff induced on a nonmagnetic atom is dominated by the valence contribution, which is known from the literature<sup>6</sup> to be proportional to the small valence  $s$  magnetic moment, arising from the  $s$ - $d$  hybridization between the on-site  $s$  orbital of the impurity and the spinpolarized  $d$  orbitals of the neighboring atoms. Indeed the core  $s$  contribution to the hff in Fig. 3 is two orders of magnitude smaller than the valence one, i.e., only several kilogauss. The negative sign of the hff indicates that it is opposite in sign to the external magnetization. The largest hff is found when the Cd atom is located in the second Fe layer from the interface (Fe2); from there the hff decreases essentially in three big steps toward the Cd value in bulk bcc Co that is assumed for the (110) geometry already in the second Co layer from the interface (Co2). For the (001) geometry the Cd field exhibits in the Co slab small oscillations arising from analogous but smaller oscillations in the Co magnetic moments. They arise from Friedel like oscillations in the magnetization density, which are induced by the perturbation due to the interfaces.

For a better understanding of the Cd hff shown in Fig. 3, we present in Fig. 4 calculations for a Cd impurity in a bulk bcc Co matrix. Here we progressively substitute the Co atoms in the first and then in the second shell around the Cd impurity with Fe atoms (open circles), focussing the attention to the change of the hff with the number of neighboring Fe atoms. For each configuration a self-consistent calculation is carried out, allowing a cluster of three shells around the impurity to be perturbed. Figure 4 clearly shows that the Cd hff scales more or less linearly with the number of Fe atoms in the first and second shell and is thus basically independent of the interaction and exact local arrangement of the Fe atoms. Starting from the Cd value in bulk Co ( $\sim -160$  kG), the induced hff of Cd increases (in absolute value) and reaches with the filling of the two shells a value which is already larger than the one attained by a Cd impurity in bulk Fe ( $\sim -290$  kG; see Fig. 3). This can be easily explained since the Fe atoms inserted in the first two shells are in

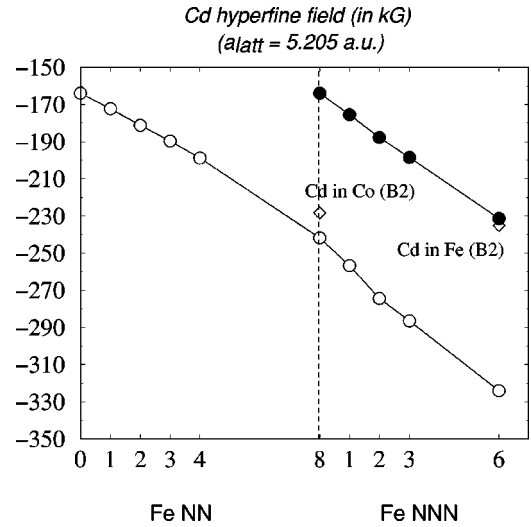


FIG. 4. Cd hff in a Co matrix as a function of the number of neighboring Fe atoms. At first the Cd atom is placed in bcc bulk Co (first left value for zero Fe neighbors of  $-164$  kG) and then the Co atoms in the first and second shells around the Cd atom are replaced one by one by Fe atoms (open circles). The filled circles refer to filling only the second shell with Fe atoms. The hyperfine fields of a Cd impurity at Co (Fe) site in a B2, i.e., CsCl structure, ordered  $\text{Fe}_{50\%}\text{Co}_{50\%}$  alloy are also reported (open diamonds).

reality still embedded in the Co matrix; in agreement with the Slater Pauling curve for the FeCo alloys, their magnetic moments are thus enhanced due to the presence of the neighboring Co atoms and so is their transferred hff to the central Cd atom. A closer inspection of Fig. 4 shows that the second shell (6 atoms) gives an even bigger contribution than the first shell (8 atoms); this unexpected behavior is to a large extent a peculiarity of the bcc structure where the second shell of atoms is not much more distant ( $1 a_{latt}$ ) than the first one ( $0.866 a_{latt}$ ). A large contribution of the second shell even remains, if we substitute only the Co atoms in the second shell by Fe atoms, thus retaining the Co occupancies in the first shell (see Fig. 4). In this case the contribution of the second shell of Fe atoms is only slightly decreased. Our calculations show that Fe atoms in the third shell have a negligible contribution to the Cd hff (less than 1 kG/atom) so that to a good extent we can limit our discussions to the first two shells. With this simple *two-shell* model, we can now understand qualitatively the different behavior of the Cd hff at the (001) and (110) Fe/Co interface shown in Fig. 3. In the bcc environment a Cd atom sitting in the Co1 layer has, in the (001) geometry, four first nn Fe atoms in the Fe1 layer and only one nnn in the Fe2 layer, which has a considerably smaller moment than the Fe1 atoms. In the (110) geometry, the Cd atom has two nn and two nnn all of them sitting in the “high moment” Fe1 layer; for this reason in the (110) geometry the “transferred” contribution is bigger than in the (001) geometry.

In Fig. 4 we report also results for the Cd atom in a substitutional Co or Fe position of an ordered FeCo alloy with B2 (CsCl) structure. In the B2 structure a Fe (Co) atom has in its nearest neighbor shell only Co (Fe) atoms and in

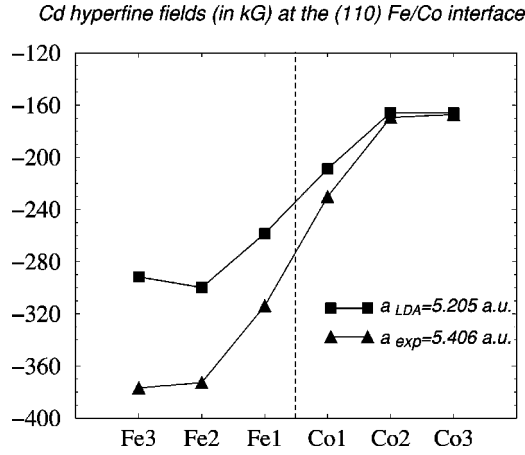


FIG. 5. Cd hyperfine field at the (110) Fe/Co interface calculated by using the LDA ( $a_{latt}=5.205$  a.u., filled squares) and experimental ( $a_{latt}=5.406$  a.u., filled triangles) lattice constant of bcc Fe.

the second and third shell only Fe (Co) atoms. Limiting us to the first two shells, a Cd atom in a Co position “Cd in Co (B2)” must therefore have a similar hyperfine field as a Cd atom in bulk Co, when the first shell is filled with Fe atoms; analogously the hff of a Cd atom in a Fe position “Cd in Fe (B2)” should have a similar hyperfine field as a Cd atom in bulk Co with the second shell filled by Fe atoms. This is indeed the case as shown in Fig. 4, indicating that the induced hff on the Cd atom is only sensitive to the magnetic environment in the first two surrounding shells.

All of the above calculations were performed by using the lattice constant of Fe ( $a_{latt}^{LDA}=5.205$  a.u.) as obtained in the LDA from the minimum of the total energy. As anticipated in the preceding section, larger Fe moments and therefore also larger transferred hff should be obtained, if the larger experimental Fe lattice constant ( $a_{latt}^{EXP}=5.406$  a.u.) is used. In order to verify this we compare in Fig. 5, for the (110) orientation, the Cd hff obtained by using both the “theoretical” and the experimental Fe lattice constant for the (110) Fe/Co interface. A substantial increment for the Cd hff in the Fe side is found, while for the Cd in Co environment the hff values do practically not change, due to the almost saturated Co moments. It is worth to note here that the increment in the Cd hff value in bulk Fe is about 28% while the change in the bulk Fe magnetic moment (see Fig. 2) is only 8%, i.e.,  $2.25\mu_B$  instead of  $2.07\mu_B$ .

By discussing possible sources of error in the calculation, we have to mention that the generalized-gradient approximation exchange-correlation functional was shown not to improve (as long as the correct lattice constant is used) the agreement with the experiments.<sup>33</sup> On the other hand, since the Cd atom has a larger size than Fe and Co atoms, relaxation around the Cd are expected in the system; a recent calculation of such relaxations for Cd impurities in Fe bulk<sup>7</sup> leads an outward relaxation of 4.3% of the nearest-neighbor distance and increases the hyperfine field by  $\sim -15$  kG (5%). Also relativistic correction arising from non- $s$  contributions (orbital and dipolar terms) are not expected to play a role. For instance the small spin moment means that the or-

bita moment is vanishing small, what we have indeed verified in fully relativistic calculations.

## V. COMPARISON WITH THE EXPERIMENTS

We can now proceed to the comparison of the calculated Cd hyperfine fields with the ones measured by the PAC experiment of Swinnen.<sup>13</sup> Experimentally, two main peaks are observed in the spectra, at  $-161$  kG and  $-381$  kG; they are attributed respectively to Cd in bcc bulk Co and Cd in bcc bulk Fe. The theoretical values, deduced from Fig. 5, agree very well with the experimental values if the experimental lattice constant is chosen, leading to  $-167$  kG and  $-377$  kG, respectively. Additional satellite fields are observed in the PAC spectra only several kG’s away from the main peaks, in detail at  $-156$  kG and  $-172$  kG for the Co environment, and at  $-387$  kG and  $-398$  kG around the Fe main peak. These satellite fields are attributed to Cd probe atoms either in Fe and Co layers in plateaus near a “sharp” Fe/Co interface. As we can see from our calculations in Fig. 3, if the Cd atom resides at the Fe1 or Co1 interface layers, the shift from the “bulk like” configurations is an order of magnitude larger, i.e., in both cases about 60–70 kG. Therefore our calculations are sufficiently accurate to dismiss the interpretation of these peaks in terms of a sharp interface.

On the other hand the experiment shows no well defined peaks at the two frequencies calculated by us for the sharp Fe/Co interface, located at about  $\frac{1}{3}$  and  $\frac{2}{3}$  of the distance between the two peaks for Cd in bulk Fe and Cd in bulk Co (with some courage, one might locate two small peaks at the expected positions in the spectrum presented in Ref. 13, only slightly peaking out-off the diffuse background). As the main result of this paper we conclude therefore that the Fe/Co interface is microscopically strongly interdiffused, in contrast to the conclusion in Ref. 13. In order to support this we have performed a total energy calculation for the exchange of a single Fe1 atom with a single Co1 atom that in line with our assumption requires a very small energy of 8 mRy = 0.11 eV. Moreover we have studied, how the Cd hyperfine field in the Co1 and Fe1 layer would be effected by a single “wrong” Fe and Co atom. As is shown in Fig. 6, the Cd hff on the Co1 layer changes by  $+4$  kG, if a Co atom is inserted as a nearest neighbor in the Fe1 layer, while the Cd hff on the Fe1 layer changes due to an additional nn Fe-atom in the Co1 layer by  $-12$  kG. This is qualitatively in line with the coordination dependence of the Cd hff discussed in Fig. 4. According to this even somewhat larger changes should result, if we introduce the additional Fe or Co atom on a nnn site (with respect of the Cd atom at the interface). What do we expect from this for the case of strong interdiffusion? The Cd probe will see a broad distribution in the occupancies of the nn and nnn sites with Co or Fe atoms, so that the configurations Fe1 and Co1 for the sharp interface will loose their dominant weights and the Fe1 and Co1 hff peaks of Cd will disappear. Due to the linear dependence of the Cd hff on the occupation numbers, they will be replaced by more or less continuous spectrum of hff basically extending between the bulk Co and bulk Fe hyperfine field values of Cd. This is compatible with the experimental results and supports our

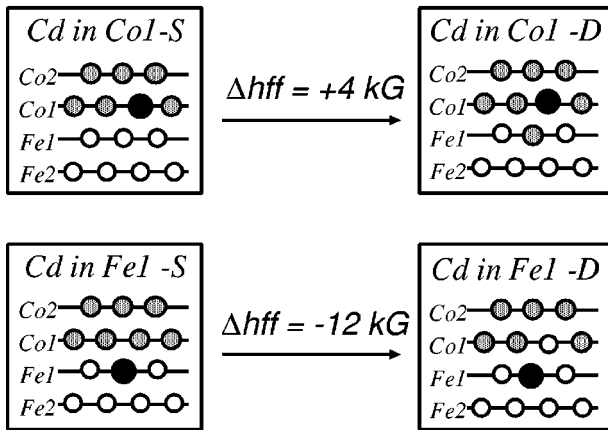
*Cd at the (110) Fe/Co interface*

FIG. 6. In the presence of a diffused atom (*D* configurations) the hyperfine fields at the sharp interface (*S* configurations) shifted in the direction as determined by the coordination numbers. The above results refer to the LDA lattice constant of Fe.

above claim being based on the nonobservation of the Fe1 and Co1 peaks of the sharp interface.

The problem remaining concerns the interpretation of the sharp satellites observed in the experiments close to the Cd hff in bulk Co and in bulk Fe. Since the deviations from the main lines are small, it seems to be natural to assume that satellites arise from Cd probes in slightly perturbed bulk Co and bulk Fe environments. Thus one could think of an Fe impurity as nn or nnn of the Cd probe atom in bulk Co, which according to Fig. 4 changes the Cd hff by  $-8$  kG as nn and  $-11$  kG as nnn. A similar argument can be put forward for a Co impurity as nn or nnn of the Cd probe in bulk Fe. On the other hand one has to consider here also the limitation of the LDA, which clearly shows up in the different hyperfine field curves of Fig. 5 as calculated for the experimental and the LDA lattice constant. This also means that in a more accurate calculation lattice relaxations both for the Co layers as well as for the Cd impurity would have to be considered. Dipolar terms should also be included, etc. In short the present calculations do not allow to make unambiguous conclusions about the origin of the satellites since the corresponding shifts are small and could have various origins.

## VI. SUMMARY AND CONCLUSION

We performed *ab initio* calculations for the magnetic properties at sharp Fe/Co bcc (001) and (110) interfaces, using the Korringa-Kohn-Rostoker Green's-function method. The magnetic moment profile at the interface agrees with previous theoretical calculations and disagrees with the profile proposed in a recent PAC experiment of Swinnen,<sup>13</sup> where using the Stearns model the magnetic moments at the interface are fitted to the measured satellite hyperfine fields induced on implanted Cd atoms at Fe/Co multilayers. In contrast to the experiments, where large oscillations approaching the interface region are claimed both at the Fe and Co sides of the interface, the calculated magnetic profiles show a monotonic increase on the Fe side and almost a constant value at the Co side of the interface. In order to compare directly to the measured quantity, we performed impurity calculations of Cd probe atoms at the Fe/Co interface, and focused our attention to the hyperfine fields induced on the Cd atoms. While the Cd hyperfine field in “bulk” bcc Fe or Co magnetic configurations is found to agree well with the experimental values (on condition that the experimental bcc Fe lattice constant is used in the calculations), the hyperfine fields induced on Cd atoms sitting at the Fe and Co interface layers are found to differ strongly from the experimental hff values of the satellites. In our calculations the Cd hyperfine fields in the interfacial Fe and Co layers are found to be about 60–70 kG away from the respective Cd values in “bulk” Fe or Co, thus lying around  $\frac{1}{3}$  and  $\frac{2}{3}$  of the distance between the Cd values in bulk Fe and in bulk Co.

From the nonexistence of these peaks in the experimental spectra we conclude that patches of nearly sharp interfaces can exist only in small amount and that the Fe/Co (110) interfaces investigated by Swinnen *et al.*<sup>13</sup> are strongly interdiffused leading to a continuous spectrum of hyperfine fields between the values of Cd in bulk Co and Cd in bulk Fe. We also conclude that our calculated results very likely exclude the possibility that the observed satellites arise from nearly ideal interface regions. Thus the experiment of Swinnen *et al.*<sup>13</sup> does not allow conclusions about the Cd hyperfine fields and the moment distribution at the *sharp* Fe/Co interface.

## ACKNOWLEDGMENT

We gratefully acknowledge valuable discussions with Professor H. Akai and Dr. B. Nonas.

<sup>1</sup>K.S. Krane, *Hyperfine Interact.* **15-16**, 1069 (1983).

<sup>2</sup>G. Schatz, in *Nuclear Physics Application on Materials Science, NMR*, edited by E. Recknagel and J. C. Soares (Kluwer, Dordrecht, 1988), p. 297.

<sup>3</sup>B.-U. Runge, M. Dippel, G. Filleböck, K. Jacobs, U. Kohl, and G. Schatz, *Phys. Rev. Lett.* **79**, 3054 (1997).

<sup>4</sup>H. Akai, M. Akai, S. Blügel, B. Drittler, H. Ebert, K. Terakura, R. Zeller, and P. H. Dederichs, *Prog. Theor. Phys. Suppl.* **101**, 11 (1990).

<sup>5</sup>G.Y. Guo and H. Ebert, *Phys. Rev. B* **53**, 2492 (1996).

<sup>6</sup>S. Blügel, H. Akai, R. Zeller, and P.H. Dederichs, *Phys. Rev. B* **35**, 3271 (1987).

<sup>7</sup>T. Korhonen, A. Settels, N. Papanikolaou, R. Zeller, and P. H. Dederichs, *Phys. Rev. B* **62**, 452 (2000).

<sup>8</sup>P. Mavropoulos, N. Stefanou, B. Nonas, R. Zeller, and P. H. Dederichs, *Phys. Rev. Lett.* **81**, 1505 (1998).

<sup>9</sup>P. Blaha, K. Schwarz, and P.H. Dederichs, *Phys. Rev. B* **37**, 2792 (1988).

<sup>10</sup>U. Gerstmann, M. Amkreutz, and H. Overhof, *Phys. Status Solidi B* **217**, 665 (2000).

- <sup>11</sup>A. Settels, T. Korhonen, N. Papanikolaou, R. Zeller, and P. H. Dederichs, Phys. Rev. Lett. **83**, 4369 (1999).
- <sup>12</sup>G.A. Prinz, Phys. Rev. Lett. **54**, 1051 (1985).
- <sup>13</sup>B. Swinnen, J. Meersschart, J. Dekoster, G. Langouche, S. Cottenier, S. Demuyne, and M. Rots, Phys. Rev. Lett. **78**, 362 (1997); **80**, 1569 (1998).
- <sup>14</sup>M.B. Stearns, Phys. Rev. B **8**, 4383 (1973).
- <sup>15</sup>Ž.V. Šljivančanin and F.R. Vukajlović, Phys. Rev. Lett. **80**, 1568 (1998).
- <sup>16</sup>A.M.N. Niklasson, B. Johansson, and H.L. Skriver, Phys. Rev. B **59**, 6373 (1999).
- <sup>17</sup>B. Drittler, N. Stefanou, S. Blügel, R. Zeller, and P. H. Dederichs, Phys. Rev. B **40**, 8203 (1989).
- <sup>18</sup>P.H. Dederichs, R. Zeller, H. Akai, and H. Ebert, J. Magn. Magn. Mater. **100**, 241 (1991).
- <sup>19</sup>H. Ebert, H. Winter, D.D. Johnson, and F.J. Pinski, J. Phys. C **2**, 443 (1990).
- <sup>20</sup>S.L. Cunningham, Phys. Rev. B **10**, 4988 (1974).
- <sup>21</sup>H.J. Monkhorst and J.D. Pack, Phys. Rev. B **13**, 5188 (1976).
- <sup>22</sup>S.H. Vosko, L. Wilk, and N. Nusair, Can. J. Phys. **58**, 1200 (1980).
- <sup>23</sup>R. Zeller, P. H. Dederichs, B. Újfalussy, L. Szunyogh, and P. Weinberger, Phys. Rev. B **52**, 8807 (1995).
- <sup>24</sup>R. Zeller, Phys. Rev. B **55**, 9400 (1997).
- <sup>25</sup>K. Wildberger, R. Zeller, and P.H. Dederichs, Phys. Rev. B **55**, 10 074 (1997).
- <sup>26</sup>M.P.L. Sancho, J.M.L. Sancho, and J. Rubio, J. Phys. F: Met. Phys. **15**, 851 (1985).
- <sup>27</sup>R. Haydock, V. Heine, and M.J. Kelly, J. Phys. C **5**, 2845 (1972).
- <sup>28</sup>P.J. Braspenning, R. Zeller, A. Lodder, and P.H. Dederichs, Phys. Rev. B **29**, 703 (1984).
- <sup>29</sup>P.H. Dederichs, B. Drittler, and R. Zeller, in *Application of Multiple Scattering Theory to Materials Science*, edited by W.H. Butler, P.H. Dederichs, A. Gonis, and R.L. Weaver, Mater. Res. Soc. Symp. Proc. No. 253 (Material Research Society, Pittsburgh, 1992), p. 185.
- <sup>30</sup>G. Breit, Phys. Rev. **35**, 1447 (1930).
- <sup>31</sup>E. Fermi, Z. Phys. **60**, 320 (1930).
- <sup>32</sup>T. Kotani and H. Akai, J. Magn. Magn. Mater. **177-181**, 569 (1998).
- <sup>33</sup>M. Battocletti, H. Ebert, and H. Akai, Phys. Rev. B **53**, 9776 (1996).